September 2024. Horticultural Plant Journal, 10 (5): 1085–1098

Horticultural Plant Journal

Available online at www.sciencedirect.com
The journal's homepage: http://www.keaipublishing.com/en/journals/horticultural-plant-journal

Research Paper

The role of the auxin-response genes *MdGH3.1* and *MdSAUR36* in bitter pit formation in apple

Daqing Huang [1], *Wen Peng* [1], *Na Gong, Lina Qiu, Yongzhang Wang, and Haiyong Qu* [*]

College of Horticulture, Qingdao Agricultural University, Qingdao, Shandong 266109, China

Received 22 December 2022; Received in revised form 15 February 2023; Accepted 26 March 2023

Available online 10 November 2023

A B S T R A C T

Apples often exhibit bitter pits in response to metabolic disorders during ripening and storage; however, the mechanisms underlying the bitter pit (BP) development remain unclear. Here, metabolome and transcriptome analyses were performed to investigate BP pulp of 'Fuji'. Two auxin-response genes, *MdGH3.1* and *MdSAUR36*, were screened. Their expression as well as the auxin content in BP pulp were found to be higher than those in healthy pulp ($P < 0.01$). In the field, excess $CO(NH_2)_2$ increased the incidence of BP. Moreover, the auxin content and *MdGH3.1* expression increased in apples after nitrogen fertilization. On Day 30 before harvest, the two genes were transiently transferred to the fruit, and 20.69% and 23.21% of BP fruits were harvested. After 10 $\mu mol \cdot L^{-1}$ auxin was infiltrated at low pressure into postharvest fruit, the increase in *MdGH3.1* expression occurred earlier than that in *MdSAUR36*. *MdGH3.1* increased the expression of *MdSAUR36*, but *MdSAUR36* did not increase expression of *MdGH3.1*. Therefore, we suggest that *MdGH3.1* acts upstream of *MdSAUR36* during BP formation and that these genes induce BP formation by regulating auxin and phenylpropanoid biosynthesis.

Keywords: Apple; *Malus* × *domestica*; Auxin; Bitter pit; Flavonoids; Nitrogen fertilizer; Widely targeted metabolomics

1. Introduction

Apples are economically important crops that are widely cultivated in temperate regions (Cebulj et al., 2017). Fruit are prone to physiological and metabolic disorders in their later stages of maturity and during storage (Orcheski et al., 2021). The most investigated disorder is bitter pit (BP), which has been studied for more than a century; however, the mechanism underlying this condition remains elusive (Freitas et al., 2010; Cebulj et al., 2017; Falchi et al., 2017). The occurrence of BP is caused by calcium deficiency in the fruit (Wang et al., 2001; de Freitas et al., 2015; Bradleigh et al., 2016; Ning et al., 2023). Spraying calcium on the fruit has been reported to control the occurrence of bitter pits formation (Torres et al., 2017); however, some studies found that calcium spraying is not effective at reducing its occurrence (Ernani et al., 2008; Jemrić et al., 2016). Therefore, the role of calcium in the occurrence of BP formation is controversial. One of the largest obstacles in the study of BP is the prediction of its occurrence, and how it develops remains unknown. Research on apple BP has been conducted only after the condition is detected (Moggia et al., 2022); furthermore, the genes regulating BP have not been identified, and consequently, the mechanism underlying BP formation has not been elucidated.

Physiological disorders in fruit are related to a number of different factors, such as variety, nutrition, climate, maturity, field management, and storage conditions (Yahia et al., 2019). Metabolomics is the quantitative study of metabolites in an integrated life system and can reflect endogenous as well as

[1] These authors contributed equally to this work.

* Corresponding author.
E-mail address: haiyongqu@hotmail.com

Peer review under responsibility of Chinese Society of Horticultural Science (CSHS) and Institute of Vegetables and Flowers (IVF), Chinese Academy of Agricultural Sciences (CAAS)

https://doi.org/10.1016/j.hpj.2023.03.019

environmental dynamic changes (Dixon et al., 2006; Tang and Wang, 2006). Zupan et al. (2013) suggested the differences in metabolites between BP fruit and healthy fruit using a targeted metabolomics method. Our previous studies showed that numerous amyloplasts accumulated in BP pulp, while there were no amyloplasts in healthy pulp cells (Qiu et al., 2021). In the root response to gravity, amyloplasts affect auxin transport and concentration. Auxin is involved in regulating fruit maturation (Fenn and Giovannoni, 2021). Three families of genes act in response to signal transduction by auxins, namely, auxin/indole-3-acetic acid (*Aux/IAA*), small auxin up RNA (*Saur*), and Gretchen Hagen 3 glycoside hydrolase (*GH3*); these have been designated early auxin-response gene families (Yu et al., 2018). The higher the nitrogen content in the fruit, the higher the incidence of bitter pit, and there is a positive correlation (Terblanche et al., 1980; Marini et al., 2020). Therefore, at the fruit expansion stage of 'Fuji' apple, we began to apply excessive nitrogen fertilizer to the fruit trees and measured the changes in auxin, auxin response genes and main secondary metabolites during fruit development, to explore the role of auxin and related genes in the formation of BP.

2. Materials and methods

2.1. Plant materials

'Fuji' apples were collected at maturity in mid-October (180 d after pollination) in 2020, 2021 and 2022 from the Qingdao Fruit Research Institute Experimental Field, Shandong Province, China. Apples were sampled from trees cultivated for 10 years. The fruit with BP were collected, and the peels were removed. Pulp samples were divided into three groups: healthy fruit (control, Fig. S1, A–C); healthy pulp from fruit with bitter pit (BP-H); and bitter pit pulp (BP, Fig. S1, D–F). The pulp samples were immediately placed in liquid nitrogen. Six fruit samples were collected; each collection was repeated three times.

2.2. Qualitative and quantitative analysis of metabolites

The pulp samples (Control, BP-H and BP) were sent to Metware Biotechnology Co., Ltd (Wuhan, China) for UPLC–MS/MS analysis. Qualitative analysis of primary and secondary mass spectrometry data was performed based on the self-built MWDB (Metware Biotechnology Co., Ltd., Wuhan, China) and the existing public databases of mass spectroscopy such as MassBank (http://www.massbank.jp), KNAPSAcK (http://kanaya.naist.jp/KNApSAcK), and METLIN (http://metlin.scripps.edu/index.php).

The composition of metabolites in the pulp of bitter pitwas analyzed using the multiple reaction monitoring (MRM) method of triple quadrupole mass spectrometry (QqQ MS). In MRM mode, the precursor ions of the target substance were filtered by QqQ MS, while ions with dissimilar molecular weights were excluded to eliminate interference. After the MS data for the metabolites were obtained, the MS peaks were integrated and corrected using MultiQuant™ 3.0.2 (SCIEX, Framingham, MA, USA). Finally, the corresponding metabolite content was expressed as the chromatographic peak area integral.

2.3. Fertilization methods

Excessive $CO(NH_2)_2$ (Sinofert, China) was applied to fruit trees using two methods at 100, 70, and 40 d before fruit harvest (Fig. 1, A–C). The first method involved soil dressing into ditches 20 cm deep on both sides of the tree trunks, application of 2.5 kg urea [$CO(NH_2)_2$] per tree that nitrogen content of 46% into the ditches, followed by watering 5 kg and covering the ditches with soil. The second method involved an infusion dressing of a prepared urea solution (concentration 5%) that was placed in a special nutritional bag (1.5 kg per bag). Excessive nitrogen fertilizer was applied to the rootstock position of the fruit trees by infusion, and the flow rate was adjusted that each bag was infused continuously for 30 d. Normal fertilization management was used as the control. The management processes for fruit trees with excessive nitrogen application were the same as those of control fruit trees.

2.4. RNA isolation, and RNA-seq library preparation

We used (Tiangen DP411, CLB + Adlai RN40, CTAB + Adlai RN40, Tiangen DP762-T1C) kit/TRIzol kit to complete the extraction of RNA from BP-H, BP, and healthy fruit pulp for transcriptome sequencing and Beijing Biomarker Technology's

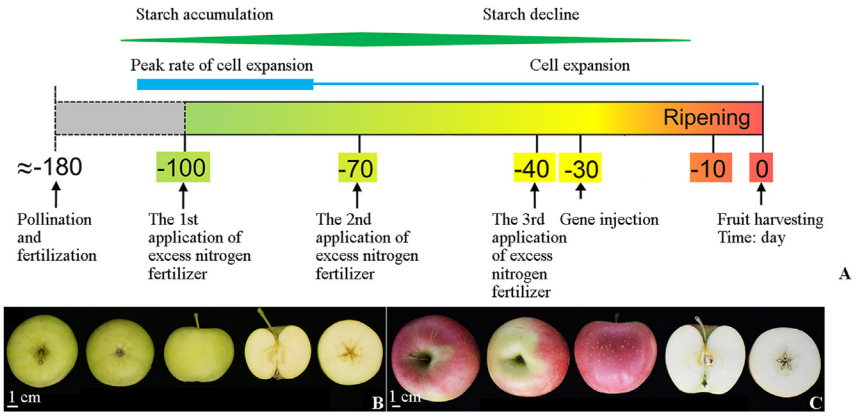

Fig. 1 Time of fertilizer treatment and gene construct injection

(A) Apples were harvested at maturation, approximately 180 d after pollination. We set the harvest time at 0 d and the number of days before harvest as negative values. Excessive nitrogen fertilizer was applied from −100 d, once every 30 d, with three applications in total. At −100 d, fruit is in the young stage, during which fruit cell volume increases and starch gradually accumulates. Vectors/gene constructs were introduced by injection at −30 d. (B) Young fruit at −100 d. (C) Ripe fruit for harvest.

(http://www.biomarker.com.cn) commercial experimental procedure for transcriptome analysis. Transcriptome data supporting the results of this study can be obtained from NCBI under BioProject number PRJNA733599 with SRA accession numbers SRR14684876, SRR14684877, and SRR14684878.

2.5. Quantitative real-time PCR to evaluate gene expression in the pulp

Samples for qRT–PCR analysis included healthy fruit, healthy BP-H, BP, pulp transformed by injection *in vivo*, and pulp treated with nitrogen fertilizer. Total RNA was extracted from pulp in liquid nitrogen using TRIzol™ reagent (Invitrogen/Thermo Fisher Scientific, Waltham, MA, USA) and reverse transcribed into (2 μg of total RNA per reaction) cDNA using an Omniscript RT kit (Qiagen, Hilden, Germany). All primers (Table S1) were synthesized at Huada (The central facility of Institute of Molecular Biology and Biotechnology, McMaster University). The efficiency of gene amplification was more than 95% using a dye-based qRT-PCR kit (Vazyme, China). Gene expression data were normalized to the expression levels of *actin* and expressed as a ratio based on the relevant controls (specified value = 1).

2.6. Phenylalanine ammonia lyase (PAL) activity assays

PAL activity assays were performed using a Phenylalanine Ammonia-lyase Activity Assay Kit from Beijing Solarbio Science & Technology Co., Ltd (Beijing, China). A total of 1 mL of borate buffe was added to a 0.1 mg pulp (Control, BP, BP-H, pulp from the injection site of *MdGH3.1* and *MdSAUR36*) and fully homogenized on ice. The samples were centrifuged at 11 000 r · min^{-1} at 4 °C for 10 min to remove insoluble materials, and the supernatants were collected on ice for testing. PAL activity was evaluated at 290 nm using a model UV1810 spectrophotometer (Shanghai Yoke Instrument Co., Ltd., Shanghai, China).

2.7. Plant flavonoid and lignin content assay

Pulps (Control, BP, BP-H, pulp from the injection site of MdGH3.1 and MdSAUR36) were dried to constant weight, pulverized through ultrasonic cell crushing apparatus (Model: SCIENTZ-IID, SCIENTZ, Nibo, China), and passed through a 40-mesh sieve. Then, the flavonoid content of 100 mg sample was determined using Plant Flavonoids Content Assay Kit (Beijing Solarbio, article number: BC1330) and the lignin content of 5 mg sample was measured using Plant Lignin Content Assay Kit (Beijing Solarbio, article number: BC4220).

2.8. Auxin content assay

Qingdao Kechuang Quality Testing Co., Ltd. was commissioned to use a plant auxin ELISA kit (MM-0953O1, Meimian Industrial Co., Ltd., Jiangsu, China) for auxin content detection. The samples (200 mg) were fully homogenized [Model: Wonbio-48P, Thundersci, Thunderscience (Shanghai) Co., Ltd., Shanghai, China], centrifuged at 5 000 r · min^{-1} for 15 min (4 °C), and then added 50 μL sample and 50 μL working solution of biotinylated antigen to the well plate. Cover it with seal plate membrane, gently shake and mix for 60 min at 37 °C incubation. Each wells inject into the wash solution (PBS buffer) 350 μL to remove biotinylated antigen, wash plate 5 times. Add the 50 μL avidin-HRP (Horse Radish Peroxidase) in Standard well and sample well and cover it with seal plate membrane, gently shake and mix for 60 min at 37 °C incubation. Washing it again 5 times. Color developing: add 50 μL Chromogen Solution A to each well and then add 50 μL Chromogen Solution B to each well as well. Incubate for 15 min at 37 °C, away from light for color developing. Add 50 μL Stop Solution (1 mol·L^{-1}) to each well to stop the reaction (the blue color changes into yellow immediately at that moment). Take blank well as zero, measure the absorbance (OD) of each well one by one under 450 nm wavelength by Microplate Reader (Model: 450, Labsystems Multiskan MS, Finland), which should be carried out within the 15 min after having added the stop solution.

2.9. Measurement of nitrogen content in apple fruit

The apple peeled pulp was stored at 80 °C in an incubator (Model: DW-86L726G, Haier, China) for 24 h. Subsequently, the dried samples were ground into powder, and the nitrogen content was measured by the DigiPREP TKN Systems (Kjeltec8400, Foss, Denmark). For each sample, 500 mg dried powder was measured, and the nitrogen content per unit fruit dried weight was calculated as a percentage.

2.10. Low-pressure infiltration treatment

In accordance with the method developed by Torres et al. (2017), Fifteen fruits were immersed in 100 μmol·L^{-1} indole-3-acetic acid (IAA) each time and repeated 3 times. A combination of 400 mmol·L^{-1} mannitol and 0.01% (v/v) Tween-20 was added to the solution (control solutions contained only mannitol and Tween-20). The fruits were treated under a pressure of 250 mm Hg for 2 min.

2.11. Transformation by injection in vivo

Using apple pulp cDNA as a template, the target gene (*MdGH3.1* and *MdSAUR36*) was cloned using a 2× Phanta® Flash Master Mix Kit (Vazyme, China). The ClonExpress® Ultra One Step Cloning Kit (Vazyme, China) was used to ligate the target gene into the expression vector pEarleyGate103, which was then transferred into *Agrobacterium tumefaciens* EHA105 (Beijing Tsingke) after verification. The cells were propagated in LB (Luria–Bertani) medium for 12 h, centrifuged at 5 000 r · min^{-1} for 5 min, collected precipitate, added appropriate MES infection solution, and adjusted OD_{600} to 0.5–0.6 for activation in MES medium for activation. Sixty apples were randomly selected for injection 30 d before fruit harvest (−30 d) *in vivo* (Fig. 1, A). Injection was performed based on the methods developed by Yasmeen et al. (2009). The injection site was close to the calyx end of the fruit. All fruit samples were injected twice on two consecutive days. Those injected with vectors lacking the target genes were used as negative controls.

2.12. Annexin V-FITC/PI staining

Apoptotic cells were assessed using the Annexin V-FITC Detection Kit (Vazyme, China) according to the manufacturer's protocol. The pulp was processed according to Qiu et al. (2021). The apoptotic index was immediately determined using a fluorescence microscope (EVOS Auto 2, Thermo Fisher, USA).

2.13. Statistical analysis

The metabolic data were analyzed using principal component analysis (PCA) to evaluate the metabolic diversity among and within samples (Wang et al., 2016). Data were standardized before analysis. Two screening criteria for differential metabolites were established, fold change 2 or 0.5 and $P < 0.05$, using Student's *t* test.

Correlation statistics, heatmap, and statistical mapping were performed using GraphPad Prism 7.0 (GraphPad Software Inc., San Diego, CA, USA). The data are expressed as the mean ± *SD*. Student's *t* test was used to analyze the differences between experimental groups. KEGG functional classification was performed using online tools from Biomarker Technologies (http://www.biocloud.net/).

3. Results

3.1. Differential metabolite analysis

A total of 445 metabolites were detected using the UPLC–MS/MS detection platform and a self-built database. The levels of these differential metabolites were generally increased in the BP tissues. However, only 28 metabolites differed between the control and BP-H groups (Fig. 2, A). These results suggest that the increase in the metabolite content is directly related to the presence of BP. The metabolite data were subjected to PCA to categorize the three types of fruit tissue based on their metabolite composition and separated the two types of healthy pulp tissue (Control and BP-H) from pulp tissue with bitter pit, while the second component (PC2) separated the two types of healthy pulp tissue (Control and BP-H). The first dimension accounted for 82.7% of the variation, whereas the second dimension only accounted for 5.5% of the variation (Fig. 2, B). The metabolite correlation coefficient between the control and BP-H groups was 0.98, whereas the correlation coefficient between the control and either BP-H or BP groups was 0.33 and 0.32, respectively (Fig. 2, C). These data suggest that major differences exist between the metabolite levels in healthy pulp tissue and BP. Moreover, the fruit exhibited metabolic changes only at the site where BP was evident.

3.2. The auxin content and PAL activity in BP pulp

Following a cluster analysis of metabolite levels among different samples, we found that the levels of phenolic acids, flavonoids, alkaloids, terpenoids, lignans, coumarins, tannins, quinones, and other metabolites were higher in the BP pulp than in healthy pulp (Fig. 3, A). KEGG pathway analysis showed that these metabolites were involved in 16 metabolic pathways (Table S2). Among these, phenylpropanoid biosynthesis, plant hormone signal transduction, and flavonoid biosynthesis were the main metabolic pathways. Plant hormone signal transduction is an environmental information process (Fig. 3, B).

Transcriptome analysis of healthy pulp and BP pulp revealed 431 differentially expressed genes (DEGs). KEGG pathway analysis showed that these DEGs were primarily associated with plant hormone signal transduction and phenylpropanoid biosynthesis (Fig. 3, C).

KEGG pathway annotation revealed that 46 genes are involved in phenylpropanoid biosynthesis, plant hormone signal transmission, and other metabolic processes. The expression of these 46 genes was evaluated using qRT-PCR. The expression of 27 genes was upregulated in BP (Fig. 4), while that of 10 genes was upregulated in healthy pulp (Fig. 4) (Corresponding to 96% and 70% of the transcriptome, respectively). This finding suggests that the results of the metabolomic analyses, transcriptome, and qRT-PCR are consistent.

The auxin levels in the control and BP-H groups were markedly lower than those in the BP group, whereas there were no differences in the auxin levels between the control and BP-H groups (Fig. 5, A). No differences in GA, ZT, ABA and SA concentrations were detected between healthy fruit pulp and BP pulp ($P > 0.05$) (Fig. S2). PAL is the key enzyme in phenylpropanoid biosynthesis pathways, and its activity was the

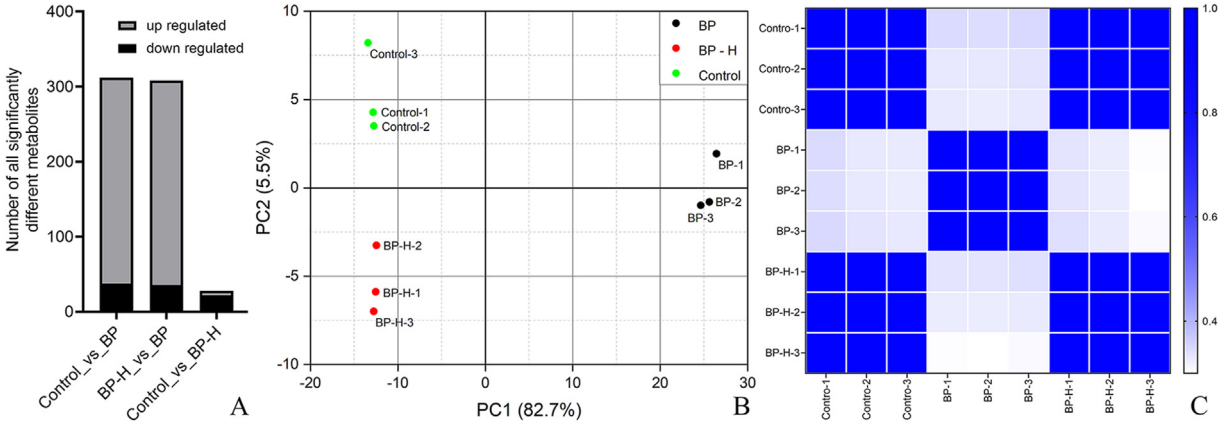

Fig. 2 Overview of the global metabolic profile of 'Fuji' apple based on three types of pulp

(A) Statistical data for the different metabolites. (B) Principal component analysis (PCA). (C) Metabolite correlation coefficients among the three types of pulp. The bar at the right shows a color code of the coefficients obtained from the analysis using pairwise Pearson's correlations. Control, BP-H, and BP refer to healthy fruit, healthy pulp obtained from bitter-pit fruit, and bitter-pit pulp, respectively.

Fig. 3 Differential metabolite clustering heatmap and KEGG classification of unigenes

(A) Sample names have been plotted on the horizontal axis, and metabolite information is plotted on the vertical axis. The different colors represent the values obtained after standardization (Color scale: red represents high content and green represents low content). (B) The differential metabolites of healthy pulp and BP pulp were classified according to the KEGG pathway. The ordinate is the KEGG metabolic pathway name, and the abscissa is the number of metabolites annotated to this pathway and its proportion to the total number of metabolites annotated. (C) Pathway enrichment analysis of 431 differentially expressed genes (DEGs). KEGG pathways have been plotted on the horizontal axis, whereas genes with KEGG items have been plotted on the vertical axis (Color scale: red represents low *P*-value and blue represents high *P*-value).

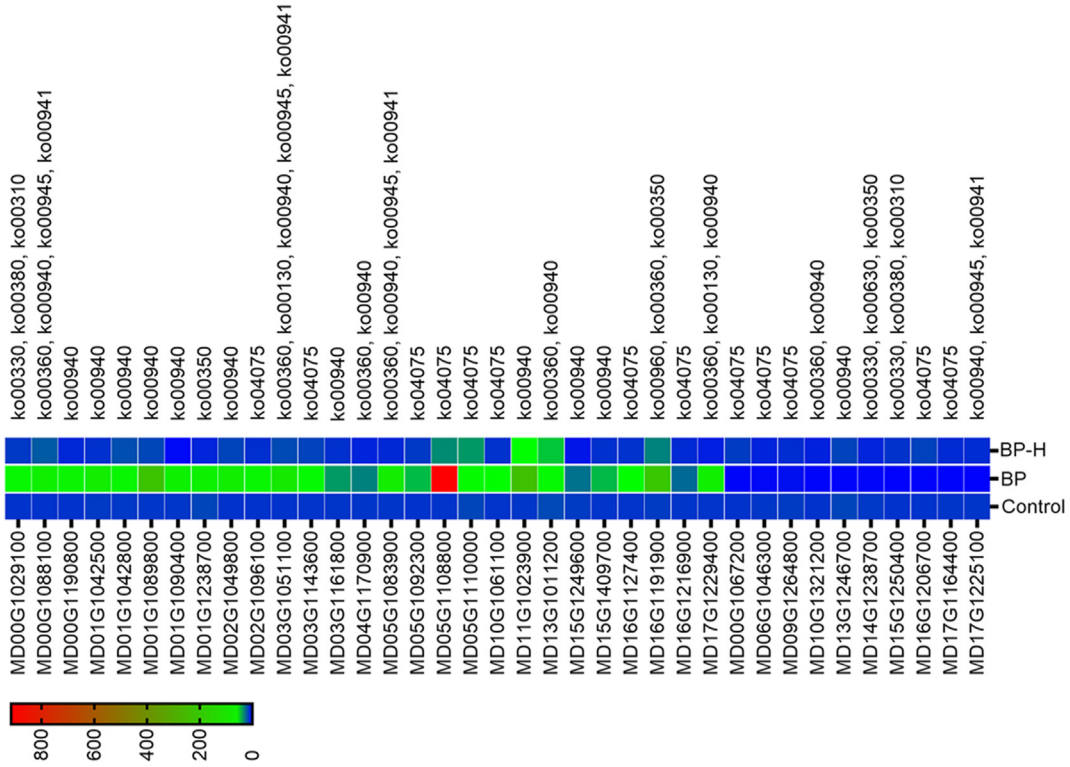

Fig. 4 Metabolic pathways involved in differentially expressed genes validated by RT-PCR

Upregulated (27) or downregulated (10) genes in the BP pulp (Color scale: red represents high expression and blue represents low expression). The 37 genes are involved in the 12 metabolic pathways.

highest in the BP pulp and the lowest in BP-H (Fig. 5, B). This finding further demonstrates that the results of metabolomic analysis were reliable. Both lignin and flavonoids are products of the phenylpropanoid biosynthesis pathway, but there are competing substrates (Vogt, 2010; Kurepa et al., 2018; Singh et al., 2019). The lignin content in BP pulp was lower than that in healthy pulp (Fig. S3), but the flavonoid content was higher than that in healthy pulp (Fig. 5, C). This result suggests that auxins and flavonoids accumulated in BP pulp, while the lignin content decreased.

3.3. *MdGH3.1 and MdSAUR36 induced BP formation in fruit in the field*

KEGG pathway analysis of 46 DEGs revealed that *MD05G1092300* is responsible for encoding GH3 in the auxin signal transduction pathway and that *MD10G1061100* corresponds to SAUR (Fig. 6, A). The 2 genes were all upregulated and expressed in BP pulp (Fig. 4) and named *MdGH3.1* and *MdSAUR36* (Table S3). In the field, the two genes were individually transferred to the pulp by injection 30 d before harvest (Fig. 1). When the fruit was harvested at maturity,

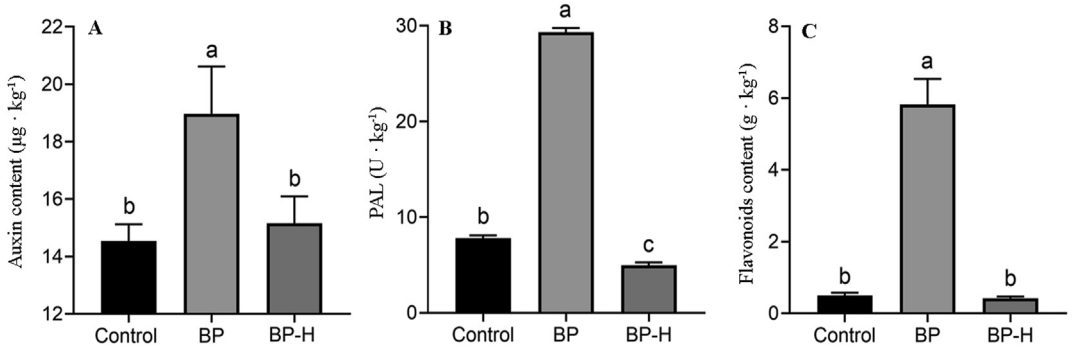

Fig. 5 The detection of auxins, PAL, and flavonoids of the phenylpropanoid biosynthesis pathway in the fruit during storage

(A) Auxin content of the pulp at the calyx end of the fruit. (B) Phenylalanine ammonia-lyase (PAL) activity at the calyx end of the fruit. (C) Flavonoid content of the pulp at the calyx end of the fruit. Control: healthy fruit; BP-H: healthy pulp obtained from bitter-pit fruit; BP: bitter-pit pulp. The different letters represent statistical significance at $P < 0.05$. Data are expressed as the mean value ± standard deviation.

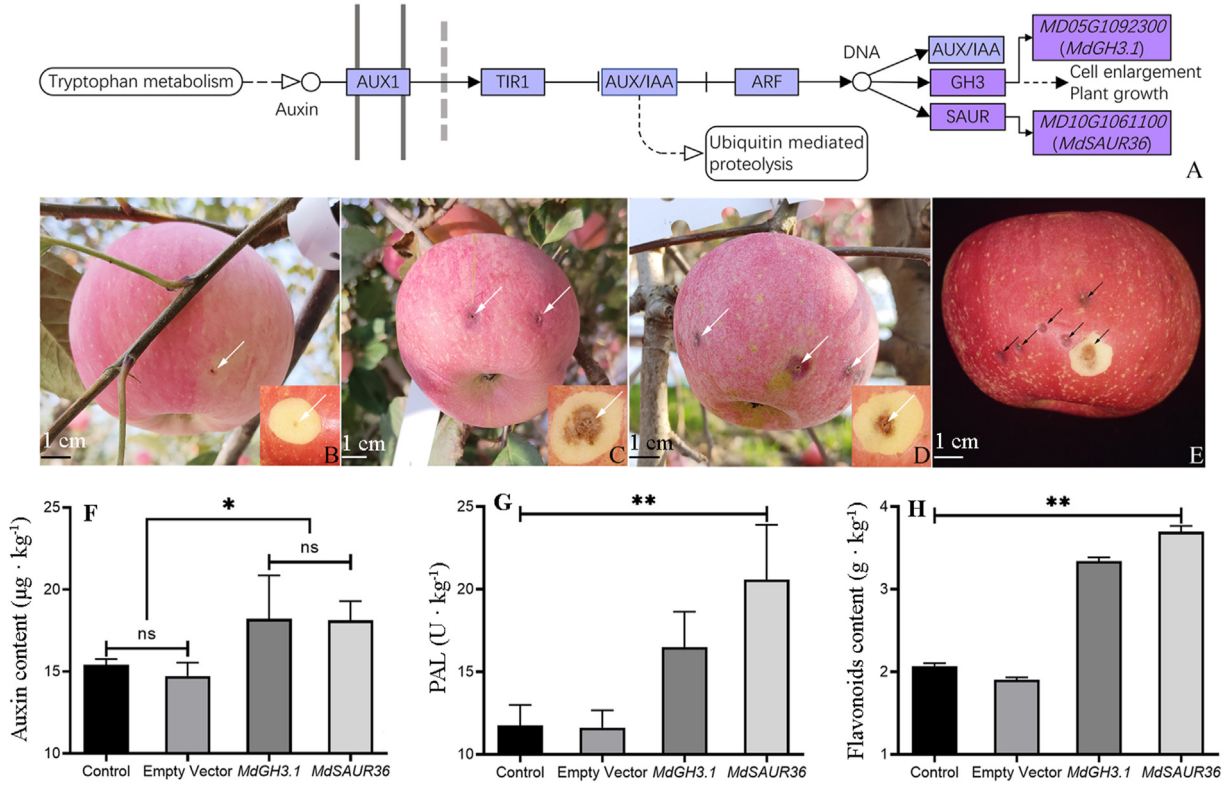

Fig. 6 Effect of injection with *MdGH3.1* and *MdSAUR36* in pulp cells at the calyx end on Day 30 before harvest (−30 d)

(A) Genes corresponding to auxin signal transduction after KEGG analysis of 431 differentially expressed genes. (B) Empty vector injection. The inner image is the pulp of the injection site (white arrow). (C) *MdGH3.1* injection. (D) *MdSAUR36* injection. (E) Naturally occurring BP fruit. A BP spot on the exocarp was removed. The black arrow indicates the site of BP. Whole apples were photographed in the field 7 d before harvest, and the inner images were photographed indoors after the wax and powder on the surface were washed after harvest. Therefore, the peel is a different color. (F) Auxin content of the pulp in the injection site. The control was healthy fruit (G) PAL activity. (H) Flavonoid content. $^{*}P < 0.05$; $^{**}P < 0.01$.

the pulp at the injection site (Fig. 6, B–D) was completely consistent with the symptoms of naturally occurring BP (Fig. 6, E and Fig. S1, D–F). The 2 genes injected into apples in the field for two consecutive years (2021 and 2022) could increase the formation rate of BP compared to the control and nitrogen fertilizer treatment (Table 1). Analysis of auxin content, PAL activity, and flavonoid content at the *MdGH3.1*- and *MdSAUR36*-injection sites showed that they were higher than those in the pulp of healthy fruit (Fig. 6, F–H). Therefore, we suggest that these two genes induce the formation of BP.

3.4. *Effects of excessive nitrogen application on the expression of MdGH3.1 and MdSAUR36*

To study the influence of nitrogen on these two genes, we applied excessive nitrogen fertilizer to fruit trees using two methods (Fig. 1). The two fertilization methods significantly increased the nitrogen content in apple fruit during harvest (Fig. S4) and the number of samples with BP (Table 1). The trend in auxin content after fertilization was opposite to that of the control fruit, especially at maturity. The auxin content of the control fruit gradually decreased, while the auxin content of the fruit with excessive nitrogen application gradually increased (Fig. 7, A). The trend in the expression of *MdGH3.1* or *MdSAUR36* in fruits exposed to the two fertilizer treatments was consistent with that in the control; however, the expression of *MdGH3.1* in the later stage of fruit development was higher than that in the control (Fig. 7, B), while the expression of *MdSAUR36* did not differ between the fertilizer treatments and the control (Fig. 7, C). As the fruit matured, PAL activity decreased rapidly; however, the PAL activity in the control fruit at maturity increased slightly, whereas that in fruit treated with nitrogen fertilizer decreased ($P < 0.05$) (Fig. 7, D). The flavonoid content in the fruit treated with nitrogen fertilizer was higher than that in the control, but the difference was not significant ($P > 0.05$) (Fig. 7, E). The auxin content, PAL activity, and flavonoid content in the pulp of BP were higher than those in healthy pulp (Fig. 5, E–G). Based on these results, we suggest excessive nitrogen application triggers changes in the fruit auxin content and increases the expression of *MdGH3.1* but has no effect on the expression of *MdSAUR36* (changes in auxin content and *MdGH3.1* are known regulatory

Table 1 The incidence (%) of apple BP with various treatments at the time of fruit harvest (2021–2022)

Treatment	2021	2022
Control	0.14 (1/690)	0 (0/592)
Soil dressing	2.09 (22/1049)	2.33 (8/343)
Infusion dressing	2.24 (32/1428)	6.54 (51/780)
Empty vector	0 (0/56)	0 (0/78)
MdGH3.1	20.69 (12/58)	23.68 (18/76)
MdSAUR36	23.21 (13/56)	31.17 (24/77)

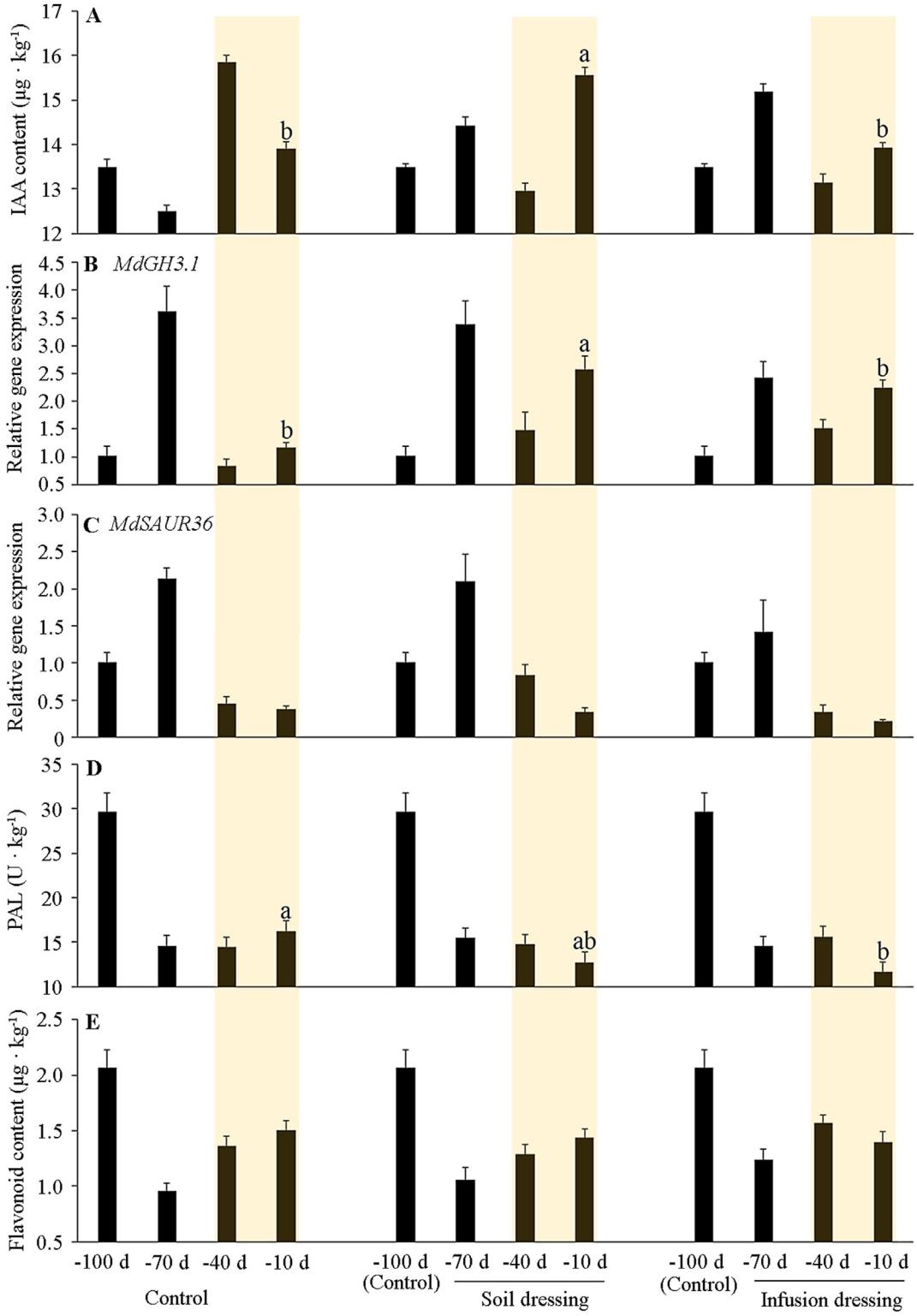

Fig. 7 Effect of excessive nitrogen fertilizer (using both soil dressing and infusion dressing on trees) 100 d before harvest (−100 d) The absence of excessive fertilizer served as a control. Auxin content, gene expression, phenylalanine ammonia-lyase (PAL) activity and flavonoid content were analyzed every 30 d. (A) Changes in auxin content in calyx pulp from 100 d before harvest (−100 d) to 10 d before harvest (−10 d). (B) Relative gene expression of *MdGH3.1* from −100 d to −10 d in response to the three treatments. (C) Changes in the expression of *MdSAUR36* from −100 d to −10 d in response to the three treatments. RGE: Relative gene expression. (D) PAL activity. (E) Flavonoid content. Different lowercase letters indicate significant differences ($P < 0.05$) for the three treatments at 10 d before harvest (−10 d), while the absence of lowercase letters indicates no significant difference between data points ($P > 0.05$).

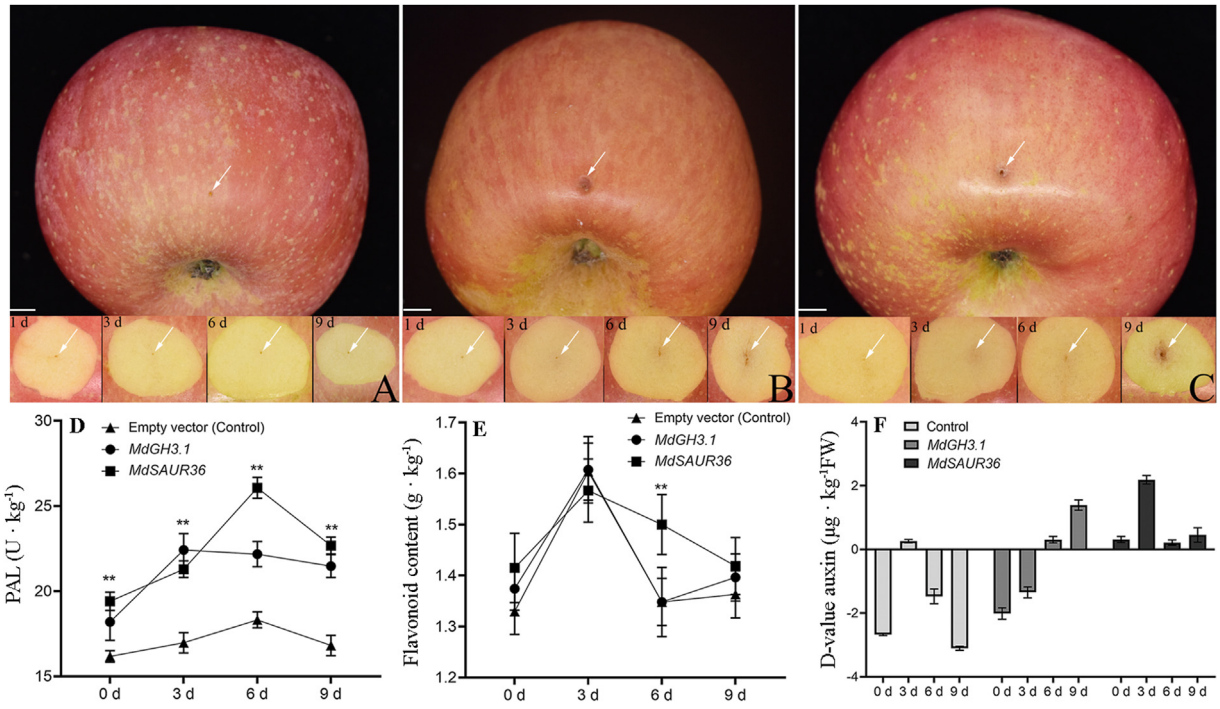

Fig. 8 Effect of injection with *MdGH3.1* or *MdSAUR36* in the pulp cells after harvest

(A) Empty vector injection. The inner image shows the color change of the pulp without the exocarp at the injection site over nine consecutive days. (B) *MdGH3.1* injection. (C) *MdSAUR36* injection. Scale bar: 1 cm. (D) Changes in phenylalanine ammonia-lyase (PAL) activity in the pulp at the injection site over nine consecutive days. The 0 d on the abscissa represents 2 h after the two genes were injected into the apple fruit. (E) Flavonoid content of the pulp at the injection site. (F) Auxin content of the pulp at the injection site. Differences were compared between data from the same day (Student's *t*-test). $^{**}P < 0.01$.

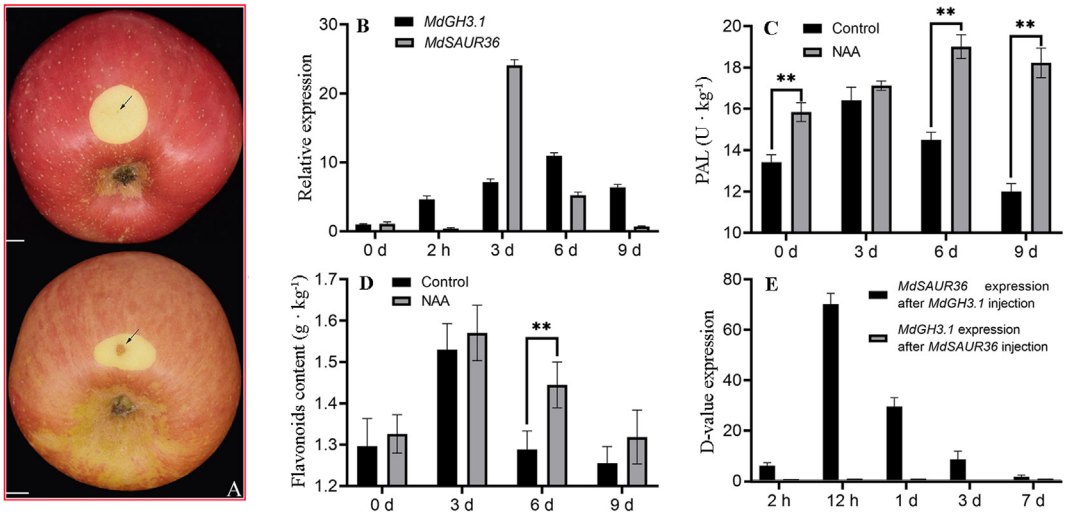

Fig. 9 Effect of auxin treatment on the apple pulp and the interaction between *MdGH3.1* and *MdSAUR36*

(A) The upper apple is water injection on 9 d (control). The black arrow indicates the injection site. The lower apple is naphthalene acetic acid (NAA) injection (100 μmol·L^{-1}) on 9 d. Scale bar: 1 cm. (B) The expression of *MdGH3.1* and *MdSAUR36* in the pulp after low-pressure penetration of auxin for 9 d. The value of 0 d in the abscissa indicates that when the apple is not injected with auxin, the relative expression of the two genes is 1. (C) Phenylalanine ammonia-lyase (PAL) activity after low-pressure penetration of auxin for 9 d. The 0 d on the abscissa represents 2 h after the two genes were injected into the fruit. (D) The flavonoid content of the pulp after low-pressure penetration of auxin for 9 d. The 0 d on the abscissa represents 2 h after the two genes were injected (E) Expression of *MdSAUR36* or *MdGH3.1* following the injection of *MdGH3.1* or *MdSAUR36* into the pulp. Differences were compared between data from the same day (Student's t-test). ** $P < 0.01$.

factors in the formation of BP); and high PAL activity and increased flavonoid content were observed after BP formation.

3.5. *Effects of MdGH3.1 and MdSAUR36 on postharvest fruit*

Harvested fruit were injected with target gene constructs. While the fruit samples injected with the empty vector did not exhibit any symptoms of BP (Fig. 8, A), 100% symptoms of BP were observed at 9 d in the fruit samples injected with the gene constructs. The color of the injection sites gradually deepened with time (Fig. 8, B and C). Both *MdGH3.1* and *MdSAUR36* increased PAL activity at the injection sites starting on the first day of injection (0 d) (Fig. 8, D). *MdGH3.1* increased the flavonoid content in the pulp, and although the average values on Days 0 and 9 were higher than those in the control, the difference was not significant (Fig. 8, E). *MdSAUR36* increased the flavonoid content only on Day 6 ($P < 0.01$); on Day 9, the content remained higher than that in the control, but the difference was not significant (Fig. 8, E). These results are consistent with those obtained for nitrogen fertilizer treatment in the field, where flavonoids are the known products of BP.

Changes in auxin concentration at the injection site were detected after injecting the gene constructs. To eliminate changes in the auxin content in response to mechanical damage to the injected pulp (Canher et al., 2020), the auxin concentration in the injected pulp was subtracted from that in the noninjected pulp, denoted Difference value auxin (D-value auxin), and this was then used to evaluate the effects of *MdGH3.1* or *MdSAUR36* on the auxin content in the pulp. The pulp at the sites where the empty vector had been injected had negative D-value auxin at all times, except at Day 3. After injection with *MdGH3.1*, D-value auxin was negative from Days 0–3 and positive from Day 6 onward (increasing continuously). However, after injection with *MdSAUR36*, D-value auxin was positive between Days 0 and 9, especially on Day 3 when it reached a maximum (Fig. 8, F). These results indicated that both genes increase the auxin concentration in pulp, with *MdSAUR36* inducing the accumulation of auxin faster than *MdGH3.1*.

3.6. *The relationship between MdGH3.1 and MdSAUR36*

We injected 100 $\mu mol \cdot L^{-1}$ naphthalene acetic acid (NAA) directly into the 30 harvested fruits, 29% of the injected parts exhibited symptoms similar to those of BP by Day 9 (Fig. 9, A). Then, we introduced 100 $\mu mol \cdot L^{-1}$ NAA into the pulp via low-pressure infiltration. Following this, changes in the expression of the genes *MdGH3.1* or *MdSAUR36* were detected. After 2 h, the expression of *MdGH3.1* began to increase, with the expression continuing to increase until Day 3. However, *MdSAUR36* expressionexhibited a delay in reaching peak, attaining its highest level at Day 3 and then declining at Days 6 and 9. These results indicated that *MdGH3.1* responded to auxin earlier than *MdSAUR36* (Fig. 9, B). PAL activity in the fruit treated with NAA was higher than that (except for Day 3) in the control pulp injected only with H_2O ($P < 0.01$) (Fig. 9, C). The flavonoid content in the NAA-treated pulp was higher than the control only on Day 6 ($P < 0.01$) (Fig. 9, D). This result is relatively consistent with that for *MdSAUR36*.

We injected the gene constructs into different parts of the same fruit, with the empty vector serving as a control. The expression of *MdSAUR36* was evaluated at the *MdGH3.1* injection site, while the expression of *MdGH3.1* was measured at the *MdSAUR36* injection site. Gene expression at the injection site where the gene was injected minus gene expression at the site where the empty vector was injected was denoted as difference value expression (D-value expression). *MdGH3.1* rapidly induced the expression of *MdSAUR36*. At 12 h, the expression of *MdSAUR36* reached its highest level and then began to decline continuously. However, *MdSAUR36* did not increase the expression of *MdGH3.1* (Fig. 9, E). This result indicates that *MdSAUR36* may function downstream of *MdGH3.1*.

3.7. *MdGH3.1 and MdSAUR36 induced programmed cell death (PCD) in pulp cells*

Our previous research (Qiu et al., 2021) showed that PCD occurred in BP pulp. After Annexin V-FITC/PI staining, fluorescence was not observed in the plasma membranes and nuclei of healthy fruit cells, whereas it was observed in the diseased fruit cells (Fig. 10, A). After dexamethasone treatment, an inducer of PCD, fluorescence was observed in the plasma membranes and nuclei of healthy fruit cells (Fig. 10, B). The pulp cells of apples with BP emitted fluorescence corresponding to both the plasma membrane and nuclei (Fig. 10, C). Fluorescence corresponding to the plasma membrane and nuclei was not observed in response to injection with the empty vector (Fig. 10, D), whereas it was observed in response to injection with *MdGH3.1* and *MdSAUR36* (Fig. 10, E and F), indicating that these two genes induced PCD in pulp cells.

4. Discussion

Metabolomics is used to conduct global analysis of low-molecular-weight metabolites, providing comprehensive information about the composition of different metabolite pools (Wang et al., 2020). The same methods that had been employed for analyzing the metabolome of 'Fuji' apples were used to analyze 'Dounan' apples, and the results were consistent with those for 'Fuji' apples (Fig. S5, A and B). Therefore, the results of metabolome analysis for BP pulp seem to be reliable. Integration of metabolome and transcriptome analyses is effective to elucidate the mechanisms underlying physiological processes in horticultural plants (Liu et al., 2019; Jiao et al., 2020). In this study, an integrated analysis revealed that two auxin-response genes, *MdGH3.1* and *MdSAUR36*, were highly expressed in BP pulp. In the field, these two genes increased the incidence of BP. Although these genes can induce the formation of BP in the field, other internal and external factors might be involved. Consequently, *MdGH3.1* and *MdSAUR36* may be key candidate genes regulating the formation of BP after harvest.

Although differences in metabolite and gene expression levels between BP and healthy pulp cells can be analyzed by metabolomic and transcriptomic methods, these techniques do not explain the mechanism underlying BP formation. Given that BP is a physiological disorder, the causative agent cannot be isolated and inoculated into the host to observe an interaction as one can explore between pathogens and hosts during the elucidation of pathogenic mechanisms (as in the case of

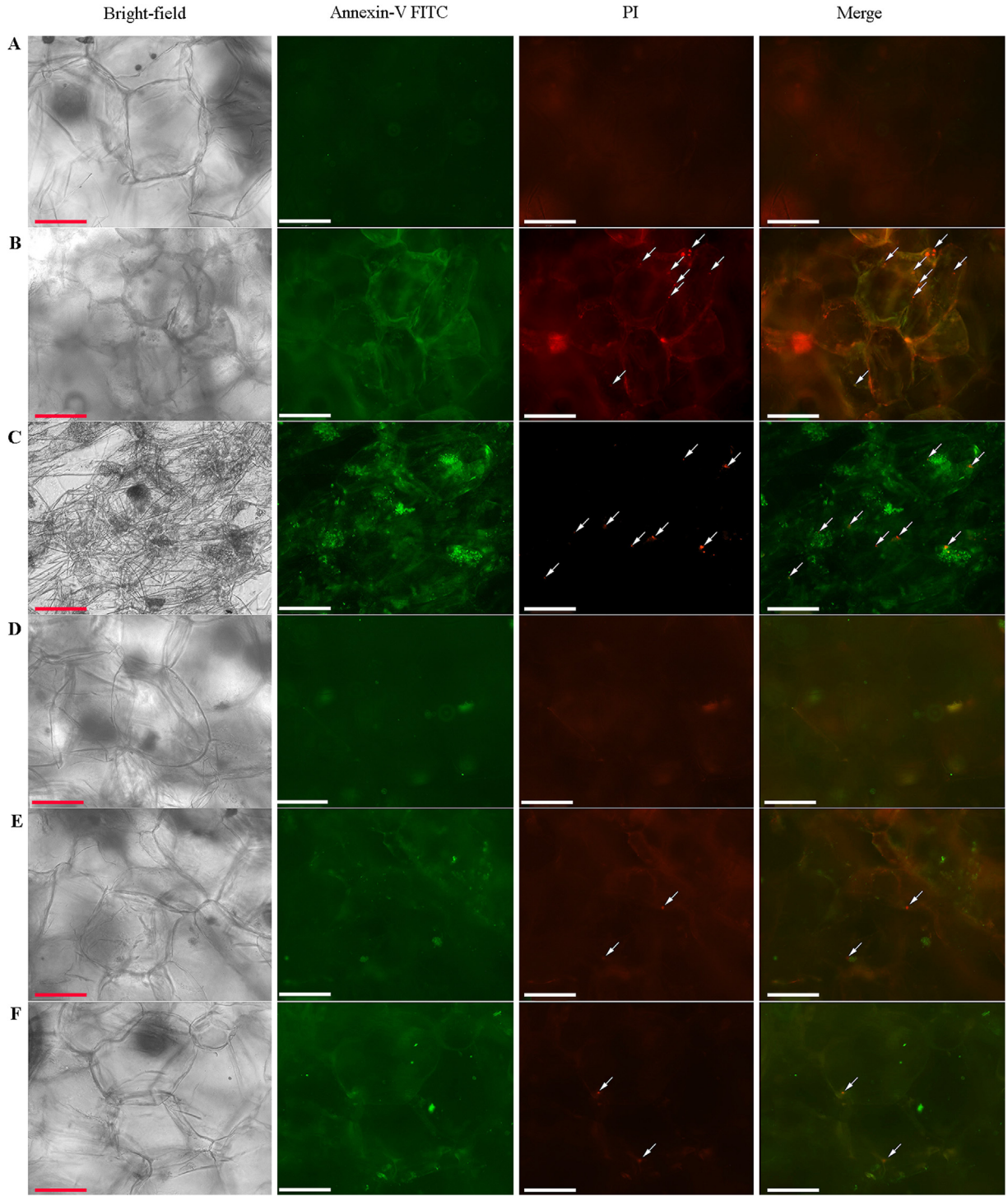

Fig. 10 Fluorescence microscopy analysis of apple pulp cells

The cells were double-stained with Annexin V-FITC (green) and PI (Propidium iodide, red). (A) Healthy pulp cell. (B) Pulp cells of an apple treated with dexamethasone. (C) Pulp cells of an apple with BP. (D) Empty vector injection at 9 d. (E) *MdGH3.1* injection at 9 d. (F) *MdSAUR36* injection at 9 d. Bright field images without fluorescence. Annexin, green channel. Green fluorescence indicates that the cell membrane was stained. PI, red channel. Red fluorescence indicates that the chromatin inside the nucleus was stained. The first three images were merged and overlaid to illustrate the corresponding structure of the stained cells. The white arrow indicates the nucleus. Magnification: 20 ×. Scar bar is 125 μm.

fungal diseases) (Büttner et al., 2021; Franco et al., 2021). It has been reported that low-pressure infiltration of $MgCl_2$ and other reagents can induce the formation of BP in other apple varieties after harvest (Moggia et al., 2022; Song et al., 2023). However, we did not use these reagents to induce BP formation in 'Fuji' apple (Fig. S6). We induced BP formation at maturity in apples through excessive application of nitrogen fertilizer in the field. Moreover, transient transformation of *MdGH3.1* or *MdSAUR36* into fruit resulted in the gradual deepening of pulp color and formation of BP.

GH3 encodes an auxin-conjugating enzyme that reduces the intracellular auxin concentration (Aoi et al., 2020; Guo et al., 2022). In this study, the expression of *MdGH3.1* increased at maturity in control fruit, while the auxin concentration began to decrease. As tomato fruit nears maturity, the expression of *GH3.1* increases and the auxin concentration decreases, thereby promoting fruit maturation (Sravankumar et al., 2018); the findings of this report are consistent with the present study. The expression of *SAUR36*, another auxin early response gene (Stortenbeker and Bemer, 2018), gradually increased during the senescence of plant leaves, thus positively regulating the process (Kanojia et al., 2021). The auxin content in leaves at the senescence stage is higher than that in the expansion stage (Hou et al., 2012). Importantly, fruit ripening is also an aging process. The present study revealed that *MdSAUR36* expression as well as auxin concentration gradually decreased during fruit ripening. The leaf area of apple trees at high altitudes (> 2 000 m) is smaller than that of low-altitude fruit trees; the auxin content was lower while the expression of *MdSAUR36* and *MdGH3.1* was higher than that in the leaves of low-altitude fruit trees (Hu et al., 2020). The low expression of *GH3* during rapid apple fruit expansion was consistent with the maximum auxin concentration at this stage (Devoghalaere et al., 2012). In this study, the expression of *MdSAUR36* and *MdGH3.1* was negatively correlated with the auxin concentration during the middle stage (−100 d to −40 d) of fruit development. However, excessive nitrogen application induced a change in the trend of auxin concentration but did not induce a change in the trend of *MdSAUR36* and *MdGH3.1* expression. These results suggest that auxins respond to nitrogen fertilizer earlier than the target genes. At maturity, the expression of *MdGH3.1* was higher in fruit trees with excessive nitrogen application than in the control, while the expression of *MdSAUR36* did not differ from the control. However, both genes were highly expressed in BP fruit, indicating that *MdGH3.1* was expressed earlier in response to auxin than *MdSAUR36* during the induction of BP. When auxin was applied, *MdGH3.1* was expressed earlier than *MdSAUR36*; moreover, *MdGH3.1* induced the expression of *MdSAUR36*, while *MdSAUR36* did not induce the expression of *MdGH3.1*, further supporting our findings.

The typical phenomenon of hybrid lethality involves seedling browning (Shiragaki et al., 2019), and PCD is involved in this process (Marubashi et al., 1999; Masuda et al., 2007; Shiragaki et al., 2020). The main reason for browning is the triggering of PAL activity by PCD, with enhanced PAL activity increasing the content of phenolic compounds (Shiragaki et al., 2020). In this study, PAL activity was also elevated in the pulp of naturally occurring BP fruit, auxin-treated fruit, and fruit injected with the target genes (*MdGH3.1* and *MdSAUR36*). Metabolomic analysis revealed that the content of phenolic compounds in the pulp of BP was higher than that in healthy pulp (Table S4); consequently, the pulp color of fruit with BP was brown. Furthermore, PCD also occurred in the pulp cells of BP fruit, auxin-treated fruit, and fruit injected with *MdGH3.1* as well as *MdSAUR36*. Therefore, we suggest that the browning process in BP pulp is consistent with that occurring due to hybrid lethality. The flavonoid contents of the pulp of naturally occurring BP and BP formed in response to the injection of target genes in the field were higher than those of healthy pulp. However, the flavonoid content at the auxin and

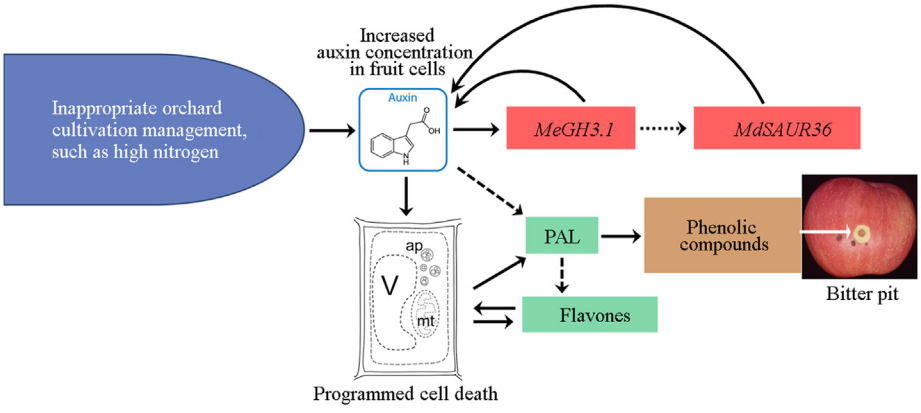

Fig. 11 Role of auxin in BP formation in apple

The auxin content, PAL activity, and flavonoid content in BP pulp were higher than those in healthy pulp ($P < 0.001$). When the auxin concentration increased, the expression of the auxin-response gene *MdGH3.1* increased, and the increased expression of *MdGH3.1* resulted in increased auxin concentration. The increased auxin concentration promoted the expression of another auxin-response gene, *MdSAUR36*, which again increased the auxin content in pulp cells. Fruit senescence is accelerated when the auxin concentration in the pulp cells continues to increase. During this process, an increase in flavonoid content serves to maintain normal programmed cell death (PCD). At the same time, PCD enhances PAL activity, which then increases the content of phenolic acids that render the pulp brown, leading to the appearance of BP symptoms. mt, mitochondrion; ap, autophagosomes; V, vacuole. Arrows with solid lines indicate a definite regulatory relationship. The dotted arrow indicates a possible regulatory relationship.

MdSAUR36 injection sites was higher than that in the control only on Day 6 after harvest. Flavonoids inhibit necrosis and promote PCD in animal cells (Vetrivel et al., 2019) as well as plant cells (Bertolini et al., 2016). Correspondingly, PCD can also induce an increase in the flavonoid content (Petrov et al., 2015; Bertolini et al., 2016). After fruit harvest, the physiological activity of the fruit decreases, with the flavonoid content decreasing substantially (Ju et al., 1996; Shamloo et al., 2013). Even when both auxin and the target genes are injected, only PAL activity and pulp browning can be increased. However, the flavonoid content increased briefly in response to auxin treatment and *MdSAUR36* injection and then decreased rapidly (Figs. 7 and 8).

In summary, our integrated metabolomic and transcriptomic analysis revealed that plant hormone signal transduction and phenylpropanoid biosynthesis are the main metabolic pathways in BP pulp (Fig. S7). Analysis of 'Fuji' apples after excessive application of nitrogen fertilizer in the field and transgenic analyses revealed that plant hormone signal transduction is involved in regulating the formation of BP; furthermore, phenylpropane metabolism was identified as the metabolic pathway that is activated after the formation of BP. Throughout fruit development, certain factors induce an increase in the levels of fruit auxin, thereby promoting the expression of *MdGH3.1*. Moreover, *MdGH3.1* also increased the expression of *MdSAUR36*, further promoting the accumulation of auxin in fruit cells. Phenylpropanoid biosynthesis is associated with auxin signaling, in concert with which it regulates plant growth and development (Lynch et al., 2020). In this study, abnormal changes in auxin in fruit pulp (such as that induced by excessive application of nitrogen fertilizer) were shown to be the cause of the changes in auxin response genes in BP fruits that are different from those observed in healthy fruits, in turn causing physiological and metabolic disorders and forming BP (Fig. 11).

Declaration of interests

The authors declare that they have no known competing financial interests or personal relationships that could haveappeared to influence the work reported in this paper.

Acknowledgments

This work was supported by the Agricultural Variety Improvement Project of Shandong Province (Grant No. 2019LZGC007), Taishan Scholar Foundation of Shandong Province (Grant No. tstp20221134) and China Agriculture Research System Foundation (Grant No. CARS-27).

Supplementary materials

Supplementary data to this article can be found online at https://doi.org/10.1016/j.hpj.2023.03.019.

REFERENCES

Aoi, Y., Tanaka, K., Cook, S.D., Hayashi, K.-I., Kasahara, H., 2020. GH3 auxin-amido synthetases alter the ratio of indole-3-acetic acid and phenylacetic acid in *Arabidopsis*. Plant Cell Physiol, 61: 596–605.

Bertolini, A., Petrussa, E., Patui, S., Zancani, M., Peresson, C., Casolo, V., Vianello, A., Braidot, E., 2016. Flavonoids and darkness lower PCD in senescing *Vitis vinifera* suspension cell cultures. BMC Plant Biol, 16: 233.

Bradleigh, H., Tyerman, S.D., Burton, R.A., Matthew, G., 2016. Fruit calcium: transport and physiology. Front Plant Sci, 7: 569.

Büttner, H., Niehs, S.P., Vandelannoote, K., Cseresnyés, Z., Dose, B., Richter, I., Gerst, R., Figge, M.T., Stinear, T.P., Pidot, S.J., Hertweck, C., 2021. Bacterial endosymbionts protect beneficial soil fungus from nematode attack. Proc Natl Acad Sci U S A, 118: e2110669118.

Canher, B., Heyman, J., Savina, M., Devendran, A., Eekhout, T., Vercauteren, I., Prinsen, E., Matosevich, R., Xu, J., Mironova, V., De Veylder, L., 2020. Rocks in the auxin stream: wound-induced auxin accumulation and *ERF115* expression synergistically drive stem cell regeneration. Proc Natl Acad Sci U S A, 117: 16667–16677.

Cebulj, A., Cunja, V., Mikulic-Petkovsek, M., Veberic, R., 2017. Importance of metabolite distribution in apple fruit. Sci Hortic-Amsterdam, 214: 214–220.

de Freitas, S.T., Do Amarante, C.V.T., Mitcham, E.J., 2015. Mechanisms regulating apple cultivar susceptibility to bitter pit. Sci Hortic-Amsterdam, 186: 54–60.

Devoghalaere, F., Doucen, T., Guitton, B., Keeling, J., Payne, W., Ling, T.J., Ross, J.J., Hallett, I.C., Gunaseelan, K., Dayatilake, G.A., Diak, R., Breen, K.C., Tustin, D.S., Costes, E., Chagné, D., Schaffer, R.J., David, K.M., 2012. A genomics approach to understanding the role of auxin in apple (*Malus* × *domestica*) fruit size control. BMC Plant Biol, 12: 7.

Dixon, R.A., Gang, D.R., Charlton, A.J., Fiehn, O., Kuiper, H.A., Reynolds, T.L., Tjeerdema, R.S., Jeffery, E.H., German, J.B., Ridley, W.P., Seiber, J.N., 2006. Applications of metabolomics in agriculture. J Agric Food Chem, 54: 8984–8994.

Ernani, P., Dias, J., Amarante, C.V.T., Ribeiro, D., Rogeri, D., 2008. Preharvest calcium sprays were not always needed to improve quality of 'Gala' apples in Brazil. Rev Bras Frutic, 30: 892–896.

Falchi, R., D'Agostin, E., Mattiello, A., Coronica, L., Spinelli, F., Costa, G., Vizzotto, G., 2017. ABA regulation of calcium-related genes and bitter pit in apple. Postharvest Biol Technol, 132: 1–6.

Fenn, M.A., Giovannoni, J.J., 2021. Phytohormones in fruit development and maturation. Plant J, 105: 446–458.

Franco, F.P., Túler, A.C., Gallan, D.Z., Gonçalves, F.G., Favaris, A.P., Peñaflor, M., Leal, W.S., Moura, D.S., Bento, J.M.S., Silva-Filho, M.C., 2021. Fungal phytopathogen modulates plant and insect responses to promote its dissemination. ISME J, 15: 3522–3533.

Freitas, S.T.D., Amarante, C.V.T.D., Labavitch, J.M., Mitcham, E.J., 2010. Cellular approach to understand bitter pit development in apple fruit. Postharvest Biol Technol, 57: 6–13.

Guo, R., Hu, Y., Aoi, Y., Hira, H., Ge, C., Dai, X., Kasahara, H., Zhao, Y., 2022. Local conjugation of auxin by the GH3 amido synthetases is required for normal development of roots and flowers in *Arabidopsis*. Biochem Bioph Res Co, 589: 16–22.

Hou, K., Wu, W., Gan, S.S., 2012. *SAUR36*, a SMALL AUXIN UP RNA gene, is involved in the promotion of leaf senescence in *Arabidopsis*. Plant Physiol, 161: 1002–1009.

Hu, D.G., Wang, N., Wang, D.H., Cheng, L., Wang, Y.X., Zhao, Y.W., Ding, J.Y., Gu, K.D., Xiao, X., Hao, Y.J., 2020. A basic/helix-loop-helix transcription factor controls leaf shape by regulating auxin signaling in apple. New Phytol, 228: 1897–1913.

Jemrić, T., Fruk, I., Radman, S., Sinkovič, L., Fruk, G., 2016. Bitter pit in apples: pre- and postharvest factors: a review. Spanish J Agric Res, 14: e08R01.

Jiao, F., Zhao, L., Wu, X., Song, Z., Li, Y., 2020. Metabolome and transcriptome analyses of the molecular mechanisms of flower color mutation in tobacco. BMC Genom, 21: 611.

Ju, Z., Yuan, Y., Liu, C., Zhan, S., Wang, M., 1996. Relationships among simple phenol, flavonoid and anthocyanin in apple fruit peel at harvest and scald susceptibility. Postharvest Biol Technol, 8: 83–93.

Kanojia, A., Shrestha, D.K., Dijkwel, P.P., 2021. Primary metabolic processes as drivers of leaf ageing. Cell Mol Life Sci, 78: 6351–6364.

Kurepa, J., Shull, T.E., Karunadasa, S.S., Smalle, J.A., 2018. Modulation of auxin and cytokinin responses by early steps of the phenylpropanoid pathway. BMC Plant Biol, 18: 278.

Liu, Y., Lv, J., Liu, Z., Wang, J., Yang, B., Chen, W., Ou, L., Dai, X., Zhang, Z., Zou, X., 2019. Integrative analysis of metabolome and transcriptome reveals the mechanism of color formation in pepper fruit (*Capsicum annuum* L.). Food Chem, 306: 125629.

Lynch, J.H., Qian, Y., Guo, L., Maoz, I., Huang, X.Q., Garcia, A.S., Louie, G., Bowman, M.E., Noel, J.P., Morgan, J.A., 2020. Modulation of auxin formation by the cytosolic phenylalanine biosynthetic pathway. Nat Chem Biol, 16: 850–856.

Marini, R.P., Baugher, T.A., Muehlbauer, M., Sherif, S., Crassweller, R., Schupp, J.R., 2020. Verification and modification of a model to predict bitter pit for 'Honeycrisp' apples. Hortscience, 55: 1882–1887.

Marubashi, W., Yamada, T., Niwa, M., 1999. Apoptosis detected in hybrids between *Nicotiana glutinosa* and *N. repanda* expressing lethality. Planta, 210: 168–171.

Masuda, Y., Yamada, T., Kuboyama, T., Marubashi, W., 2007. Identification and characterization of genes involved in hybrid lethality in hybrid tobacco cells (*Nicotiana suaveolens* × *N. tabacu*) using suppression subtractive hybridization. Plant Cell Rep, 26: 1595–1604.

Moggia, C., Bravo, M.A., Baettig, R., Valdés, M., Romero-Bravo, S., Zúñiga, M., Cornejo, J., Gosetti, F., Ballabio, D., Cabeza, R.A., Beaudry, R., Lobos, G.A., 2022. Improving bitter pit prediction by the use of X-ray fluorescence (XRF): a new approach by multivariate classification. Front Plant Sci, 13: 1033308.

Ning, Y.S., Li, H., Song, J.F., Yu, T.T., Han, M.Y., Peng, L.L., Jia, J.Q., Zhang, W.W., Yang, H.Q., 2023. Characterization of NCL family genes in *Malus* and their relationship with cellular calcium concentration in root. Acta Horticulturae Sinica, 50: 475–484. (in Chinese)

Orcheski, B., Meng, D., Bai, Y., Fei, Z., Cheng, L., 2021. The transcriptomes of healthy and bitter pit-affected 'Honeycrisp' fruit reveal genes associated with disorder development and progression. Tree Genet Genomes, 17: 37.

Petrov, V., Hille, J., Mueller-Roeber, B., Gechev, T.S., 2015. ROS-mediated abiotic stress-induced programmed cell death in plants. Front Plant Sci, 6: 69.

Qiu, L., Hu, S., Wang, Y., Qu, H., 2021. Accumulation of abnormal amyloplasts in pulp cells induces bitter pit in *Malus domestica*. Front Plant Sci, 12: 738726.

Shamloo, M., Sharifani, M., Daraei Garmakhany, A., Seifi, E., 2013. Alternation of secondary metabolites and quality attributes in Valencia Orange fruit (*Citrus sinensis*) as influenced by storage period and edible covers. J Food Sci Technol, 52: 1936–1947.

Shiragaki, K., Iizuka, T., Ichitani, K., Kuboyama, T., Morikawa, T., Oda, M., Tezuka, T., 2019. *HWA1*- and *HWA2*-mediated hybrid weakness in rice involves cell death, reactive oxygen species accumulation, and disease resistance-related gene upregulation. Plants, 8: 450.

Shiragaki, K., Nakamura, R., Nomura, S., He, H., Tezuka, T., 2020. Phenylalanine ammonia-lyase and phenolic compounds are related to hybrid lethality in the cross *Nicotiana suaveolens* × *N. tabacum*. Plant Biotechnol, 37: 327–333.

Singh, D.N., Sharma, D.D., Singh, G., Thakur, K.K., Kumari, S., 2019. Physiological Disorders and Their Management in Apple and Pear Fruits Production, vol. 3. AkiNik Publications, New Delhi, India, pp. 1–125.

Song, J., Sun, S., Wang, B., Chen, H., Shi, J., Zhang, Y., Kong, X., 2023. Fruit-stalk supplementing calcium and partition regulation of fruit calcium for prevention of bitter pit of bagged apple. J Plant Growth Regul, 42: 3000–3016.

Sravankumar, T., Akash, Naik, N., Kumar, R., 2018. A ripening-induced *SlGH3-2* gene regulates fruit ripening via adjusting auxin-ethylene levels in tomato (*Solanum lycopersicum* L.). Plant Mol Biol, 98: 455–469.

Stortenbeker, N., Bemer, M., 2018. The *SAUR* gene family: the plant's toolbox for adaptation of growth and development. J Exp Bot, 70: 17–27.

Tang, H., Wang, Y.L., 2006. Metabonomics: a revolution in progress. Prog Biochem Biophys, 33: 401–417.

Terblanche, J.H., Gürgen, K.H., Hesebeck, I., 1980. An integrated approach to orchard nutrition and bitter pit control. Acta Hortic, 92: 71–82.

Torres, E., Recasens, I., Lordan, J., Alegre, S., 2017. Combination of strategies to supply calcium and reduce bitter pit in 'Golden Delicious' apples. Sci Hortic-Amsterdam, 217: 179–188.

Vetrivel, P., Seong, M., Kim, Venkatarame Gowda Saralamma, V., Ha, S., Kim, E.H., Tae-Sun, M., Gon, S., 2019. Function of flavonoids on different types of programmed cell death and its mechanism: a review. J Biomed Res, 33: 363–370.

Vogt, T., 2010. Phenylpropanoid biosynthesis. Mol Plant, 3: 2–20.

Wang, L., Jiang, W., He, Q., Fan, H., 2001. Studies on the relationship of the development of bitter pit in apple fruits with the contents of calcium and magnesium and the activities of antioxidant enzymes. Acta Hortic Sin, 28: 200–205. (in Chinese)

Wang, R., Li, B., Lam, S.M., Shui, G., 2020. Integration of lipidomics and metabolomics for in-depth understanding of cellular mechanism and disease progression. J Genet Genomics, 47: 69–83.

Wang, S., Tu, H., Wan, J., Chen, W., Liu, X., Luo, J., Xu, J., Zhang, H., 2016. Spatio-temporal distribution and natural variation of metabolites in citrus fruits. Food Chem, 199: 8–17.

Yahia, E.M., Carrillo-López, A., Sañudo, A., 2019. Chapter 15–Physiological disorders and their control. In: Yahia, E.M. (Ed.), Postharvest Technology of Perishable Horticultural Commodities. Woodhead Publishing, pp. 499–527.

Yasmeen, A., Mirza, B., Inayatullah, S., Safdar, N., Jamil, M., Ali, S., Choudhry, M.F., 2009. In planta transformation of tomato. Plant Mol Biol Rep, 27: 20–28.

Yu, D., Qanmber, G., Lu, L., Wang, L., Li, J., Yang, Z., Liu, Z., Li, Y., Chen, Q., Mendu, V., Li, F., Yang, Z., 2018. Genome-wide analysis of cotton *GH3* subfamily II reveals functional divergence in fiber development, hormone response and plant architecture. BMC Plant Biol, 18: 350.

Zupan, A., Mikulicpetkovsek, M., Cunja, V., Stampar, F., Veberic, R., 2013. Comparison of phenolic composition of healthy apple tissues and tissues affected by bitter pit. J Agric Food Chem, 61: 12066–12071.